Phase-space singularities in atomistic planar diffusive flow

W. G. Hoover and B. Moran

*Department of Applied Science, University of California at Davis–Livermore and Lawrence Livermore National Laboratory,
Livermore, California 94550*

Morriss [Phys. Rev. A **39**, 4811 (1989)] recently published a stimulating study of a nonequilibrium Lorentz gas. He measured a multifractal "spectrum of singularities" $f(a)$ describing the "coarse-grained" phase space-representation of a time-reversible, two-body, space- and time-periodic shear flow. The measured function $f(a)$ is the "Hausdorff dimension" of attractor singularities whose local bin integrals vary as the ath power of the bin length. Morriss found a spectrum of singularities $f(a)$ very different from those familiar to nonlinear dynamical systems theory. Here we consider a closely related, but simpler, two-body time-reversible atomistic system. It is also a Lorentz-gas problem, a nonequilibrium diffusive flow, periodic in space but stationary in time. This system appears to be both mixing and ergodic, even far from equilibrium. We use the Chhabra-Jensen technique to show that the phase-space singularity spectrum $f(a)$ for this nonequilibrium flow more closely resembles those of dynamical systems theory.

I. INTRODUCTION

Molecular-dynamics simulation of nonequilibrium steady-state flows with reversible equations of motion began about 15 years ago.[1] Diffusive, viscous, and conducting flows were all simulated. Transport coefficients were generated for gases, liquids, and solids using a variety of equilibrium (fluctuation) and nonequilibrium (driven) methods. Both kinds of results were in good agreement with experimental data and the usefulness of the computer experiments was thereby established.

More recently, atomistic computer-simulation work has focused on connecting microscopic dynamical reversibility with macroscopic second-law-of-thermodynamics irreversibility in time-averaged steady states.[2] This connection has been made possible through the development of time-reversible equations of motion which describe the interaction of microscopic dynamical degrees of freedom with macroscopic heat reservoirs.[1–5]

The *mechanism* underlying second-law irreversibility lies in the Lyapunov instability of the equations of motion.[6–12] Stationary nonequilibrium flows develop by generating "multifractal" strange-attractor objects in phase space.[2,12–14] These objects have zero "volume" relative to the corresponding equilibrium states, and their phase-space "dimensionality" varies with the deviation from equilibrium. The volume collapse is rapid, on the time scale of the collision rate. The phase-space objects we study are always represented by computer-generated time series of phase-space points. The number of these points is limited by computer size and speed. Typical series contain a million to a billion points. Discrete time series *can* be analyzed directly,[15] but the coarse-grained phase-space objects analyzed by mathematicians are generally more abstract[14] static structures, consisting of uncountably many points. This difference in the data's structure can lead to misunderstanding and confusion. Because the definitions of multifractal dimensionality $\{D_q\}$ are intricate we have collected operational

definitions, appropriate to the time series we analyze here, in the Appendix. The time required to generate multifractal information is relatively long, on the time scale of Poincaré recurrence.

The simplest and most fundamental static measure of fractal phase-space dimensionality is the "information" dimension D_1. This dimension weights all points equally and corresponds to the visual information in a phase-space picture. Kaplan and Yorke conjectured that D_1 is linked to the time-averaged spectrum of dynamic Lyapunov exponents. The nature of the Lyapunov exponents, which describe the divergence and convergence of phase-space flows, has been clarified by measuring their spectrum for a variety of nonequilibrium systems. The local *time variation* of these exponents reflects the local (phase) space variation of fractal dimension. Because visualization of phase-space multifractal geometry remains difficult, we believe it is important to characterize the simplest possible systems. These simplest systems include Lorentz-gas two-body shear and diffusive flows, as well as three-body heat-conducting flows.

In a very recent and extremely stimulating paper Morriss[12] studied the multifractal spectrum of singularities $f(a)$ for a simple nonequilibrium two-body shear flow. This Lorentz-gas flow problem was introduced in 1983.[16] The two-body shear-flow problem[17] is equivalent to a one-body problem: finding the motion of a point mass moving in a constantly shearing lattice of scatterers. (The periodic geometry of the problem is indicated in Fig. 1.) Because the shear flow is periodic in time, inducing a time-periodic flow, a stationary state is never reached. Morriss found time-averaged velocity distributions that did not agree well with Boltzmann-equation predictions[18,19] as well as a multifractal singularity spectrum $f(a)$ with a cusplike structure unlike those previously characterized for maps and dynamical systems.[15,20] (See Fig. 2.)

In this paper we examine the multifractal nature of two-body isokinetic *diffusive* flow for a hard-disk Lorentz

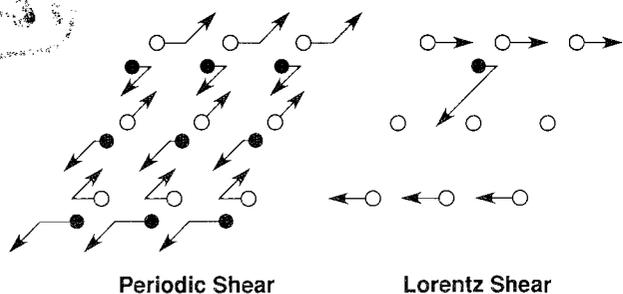**Periodic Shear** **Lorentz Shear**

FIG. 1. Two views of the geometry in the two-body shear-flow problem. The two particles interact, in Morriss's calculations, with a shifted repulsive Lennard-Jones interaction, so that the potential and its first derivative (but *not* its second derivative) are continuous. The motion is periodic in both space and time. The left view shows a symmetric two-body version in which the velocity of each particle is represented as a systematic part (horizontal component of velocity) plus a fluctuating part with the fluctuating parts summing to zero. The right view shows an equivalent one-body version in which the velocity of the filled-circle particle is taken relative to that of the open-circle particle at the origin.

gas[21−24] (also equivalent to a hundred-year-old one-body problem, the Galton board). In our isokinetic version of the Galton-board problem a single particle moves through a stationary array of fixed hard-disk scatterers under the influence of a constant external field. The motion occurs at fixed speed, imposed by applying Gauss's principle of least constraint[5,25] to the motion. The complication of time periodicity is eliminated because the boundaries do not move.

The two-body periodic problem indicated in Fig. 1 could be described in an eight-dimensional phase space $\{x,y,P_x,P_y\}$, but there are five constants of the motion (center-of-mass location, center-of-mass velocity, and kinetic energy). Thus the two-body problem can further be described in a three-dimensional phase space. The

equivalent one-body problem can likewise be described in a three-dimensional phase space including two relative space coordinates and an angle giving the direction of motion. By tabulating only the geometry of successive collisions (because the smooth trajectory between collisions can be worked out anlytically) the two problems can be reduced to two-dimensional ones. It is that approach which we follow here.

We previously found[23] that the two-dimensional cross section of the three-dimensional phase-space distribution is typically multifractal, with a "correlation dimension" D_2 between 1 and 2, but that for selected ranges of the external driving field the dimensionality drops to zero in the two-dimensional cross section, representing a stable one-dimensional limit cycle in three dimensions.

Here we analyze the multifractal phase-space singularities of this relatively simple Galton-board problem, using Chhabra and Jensen's very recent extension[20] of the ideas of Grassberger,[26] and Hentschel and Procaccia.[27]

II. MODEL AND RESULTS

The two-body field-driven isokinetic Lorentz gas produces the simplest atomistic nonequilibrium stationary state. The collisional forces are impulsive, corresponding to hard-disk collisions. Similar dynamics could be generated with very smooth forces, using functions based on $\exp(-1/r)$, but because we view the hard-disk case as simpler we study it here.

In the coordinate system of Fig. 3 (reproduced from Ref. 23) with a field of constant strength E parallel to the x axis, the Gaussian isokinetic equations of motion can be solved analytically for a particle of mass m with the constant speed P/m. The distance traveled during the interval Δt separating successive hard-disk collisions is the vector $(\Delta x, \Delta y)$:

$$\Delta x = -(P^2/mE)\ln(\sin\theta/\sin\theta_0) ,$$

$$\Delta y = -(P^2/mE)(\theta-\theta_0) ,$$

$$\Delta t = -(P/E)\ln[\tan(\theta/2)/\tan(\theta_0/2)] .$$

The angle θ gives the direction of the motion relative to the field direction
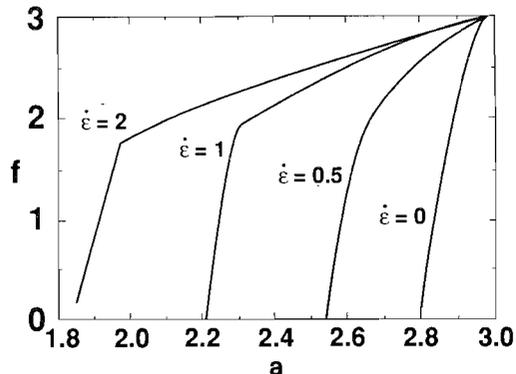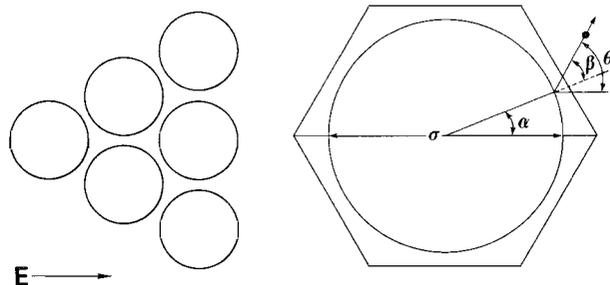
$$P_x = P\cos\theta, \quad P_y = P\sin\theta .$$

FIG. 2. Spectrum of fractal dimension found by Morriss for the system of Fig. 1 by projecting a four-dimensional phase-space distribution onto a three-dimensional subspace.

FIG. 3. Galton-board problem, showing the definition of the angles α and β which define a hard-disk collision.

To see that these one-body motion equations are *time reversible*, note that reversing a collision corresponds to replacing θ by $\theta_0 - \pi$ and θ_0 by $\theta - \pi$, correctly changing the signs of Δx and Δy without changing Δt. The motion described by these equations corresponds to that of a particle moving, at constant kinetic energy, under the influence of a field E aligned parallel to the x axis. In Hamiltonian mechanics the energy provided by the field would cause the mean kinetic energy to rise. By using a Gaussian thermostat (based on Gauss's principle of least constraint[5,25]) this energy is extracted at exactly the same rate as it is produced so that the particle "falls" (or rises) at constant speed. It has recently been shown that exactly the same (time-reversible) coordinate-space motion results from purely Hamiltonian mechanics if the field strength has an *exponential* dependence on the x coordinate.[24]

It is possible to generate 15 million collisions per hour on a CRAY-1 computer with an accuracy of seven significant figures.[23] Such calculations provide a time series of the angles α and β which describe the hard-disk collisions. If these data are accumulated in "bins" corresponding to equal numbers of increments in α and $\sin\beta$, with linear dimensions proportional to the "bin size" δ, then the *fractal spectrum of singularities f(a)* can be calculated by working out the limiting bin-size dependence of the one-parameter family of sums over bins:

$$D_q = \left[\ln \sum p^q \right] \Big/ (\ln \delta^{q-1}) \; ,$$

where q can be positive, negative, or zero. These sums, in the limit that δ becomes sufficiently small, approach corresponding integrals of singular coarse-grained probability densities. The integrated bin probability p for sampling a particular bin centered on $(\alpha, \sin\beta)$ is normalized, with the sum over bins, $\sum p = 1$. Chhabra and Jensen[20] discuss the singularities of the integrated bin probability. For sufficiently small bins the singularity is local, with integrated probability varying as the ath power of the bin size δ. Chhabra and Jensen showed that "singularity strength" a (here denoted by a rather than α to avoid confusion with the angle defined in Fig. 3) and the corresponding singularity spectrum $f(a)$ can both be determined directly from the family of q-dependent normalized probability measures $\mu_q = p^q / \sum p^q$:

$$f = \langle \ln(\mu_q) \rangle_q / \ln\delta \; ,$$

$$a = \langle \ln(p) \rangle_q / \ln\delta = \langle \ln(\mu_1) \rangle_q / \ln\delta \; ,$$

where the angular brackets indicate sums weighted with the q-dependent measure μ_q.

The geometric meaning of the singularity spectrum is intricate. We again refer to the Appendix for more details of multifractal dimensionality. The main idea is to consider a stationary phase-space attractor as a family of superposed or "interwoven" sets of singular fractal objects. In the neighborhood of any part of the attractor the integrated (coarse-grained) small-δ probability is typically singular, varying as the ath power of the bin size δ. For an attractor (as opposed to repeller) this power is typically less than the embedding dimension, signifying

the shrinkage associated with dissipation. The set of bins with the same singular probability dependence has a limiting Hausdorff bin-counting dimension $f(a)$. This means that the number of occupied bins of singularity strength a varies as $\delta^{-f(a)}$, for small δ.

To study the fractal dimension of the singularities $f(a)$ for a typical nonequilibrium situation we arbitrarily chose a field strength of $E = 3P^2 / m\sigma$ for detailed investigation. P/m is the constant speed, and σ is the scatterer diameter, chosen arbitrarily to give a scatterer density of four-fifths the close-packed value. Numerical work[23] suggests that the motion is chaotic on a strange attractor without any regular regions. The dynamical evolution generates a fractal object. We characterize the *multifractal* dimension using a range of q from 0 to 10. Outside this range the results are relatively slow to converge. A typical multifractal cross section is shown in Fig. 4. The cross section shown there has[23] an apparent *correlation* dimension D_2 of about 1.6. This means that the number of pairs of time-series points within a distance δ of each other varies as $\delta^{-1.6}$. From the visual standpoint the *information* dimension D_1 is more relevant. For this same attractor the information dimension D_1 is approximately 1.8, meaning that the number of time-series points within a distance δ of an arbitrary point (not necessarily a point on the attractor) varies as $\delta^{-1.8}$. Cross-section dimensionalities of 1.6 and 1.8 correspond to phase-space-object dimensionalities of 2.6 and 2.8.

Because the motion between collisions proceeds smoothly, the analysis of the singularities in the three-dimensional phase-space probability density reduces to a two-dimensional analysis normal to that motion. The motion can be described as a time series of $(\alpha, \sin\beta)$ pairs describing the position and relative velocity of successive collisions. The motion normal to the $(\alpha, \sin\beta)$ plane cor-
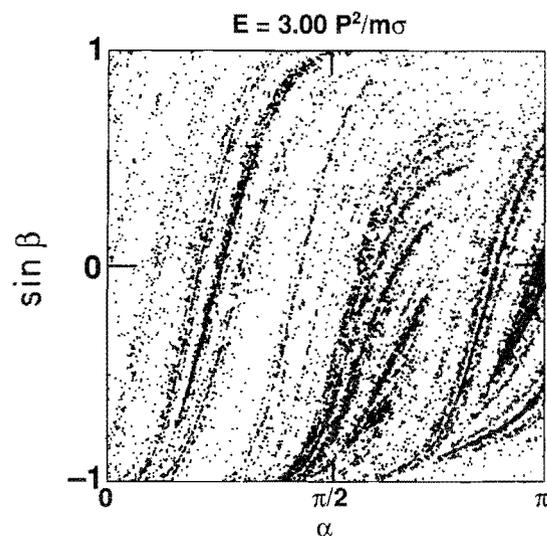

FIG. 4. Multifractal phase-space probability-density cross section found for a field strength of $3P^2/m\sigma$. The 10 000 dots shown represent 10 000 successive collisions. The calculations used in the text incorporate 100 000 000 such collisions.

responds to the time between successive collisions. This function is piecewise smooth. The variation in collision times, from the shortest possible to the longest possible free paths, is typically a factor of 10. In the equilibrium case, the relative weight of a differential element of area in the $(\alpha, \sin\beta)$ plane $d\alpha d\sin\beta = d\alpha \cos\beta d\beta$ gives the relative frequency of collision at (α, β).

To implement the ideas of Morriss, Chhabra, and Jensen we spanned the $(\alpha, \sin\beta)$ space by a 1024×1024 grid and accumulated occupation probabilities over a sequence of one hundred million hard-disk collisions. To suggest the improved resolution over that shown in Fig. 4, we show 640 000 points on an 8×8 grid in Fig. 5. With the corresponding bin probabilities we could then calculate the singularity strength $a(q)$ and its fractal dimension $f(q)$ using the Chhabra-Jensen recipe given above. (See Fig. 6.) We found that convergence is rapid for q corresponding to the information dimension ($q = 1$) and the correlation dimension ($q = 2$), as well as for larger q, up to about 5, which describes the clustering tendency of triplets, quadruplets, and quintuplets of phase-space points. Convergence for $q = 10$ is relatively slow.

Smaller values of q emphasize the less frequently visited parts of the attractor. Of the corresponding dimensions, D_0 the capacity or "box-counting" dimension which approximates the Hausdorff dimension, has an apparently simple meaning. It gives the dependence of the number of cells visited on bin size, with the logarithm of this number varying as $-D_0 \ln\delta$. D_0 is relatively more delicate to compute and slower to converge than D_1 or D_2. (See again the Appendix.) For a fixed number of col-
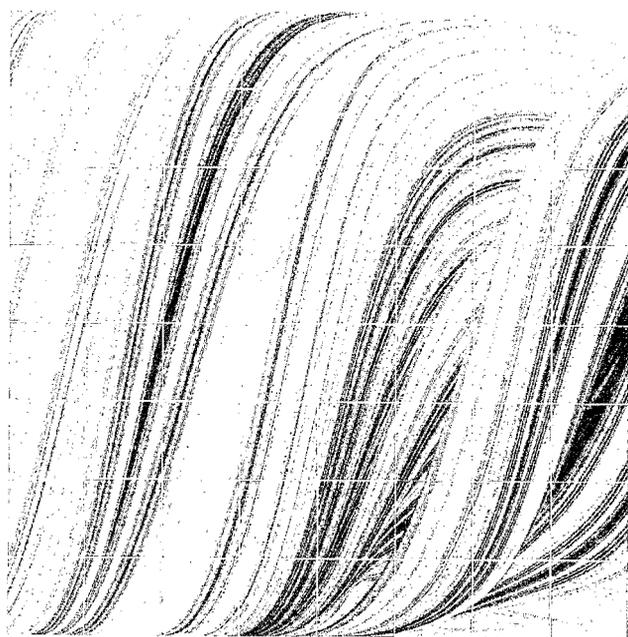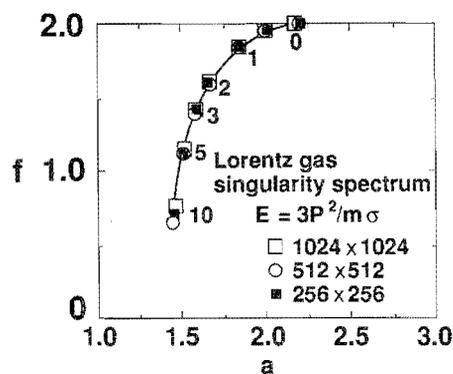

FIG. 6. Spectrum of fractal dimension $f(a)$ found here for the nonequilibrium system of Figs. 4 and 5 using a field strength of $3P^2/m\sigma$ and 100 000 000 collisions. Points shown are labeled according to the number of bins spanning $(\alpha, \sin\beta)$ space, 256^2, 512^2, and 1024^2. The q values, in the range from 0 to 10 are indicated, except for $q = \frac{1}{2}$.

lisions a sufficiently refined grid can always lead to a vanishing fraction of occupied bins, and hence to a vanishing D_0. We found that for a practicable fixed grid (that is, up to 1024×1024 bins) we could occupy nearly all the bins.

It appears that *every bin would become occupied* provided that sufficiently many collisions could be generated, though we were unable actually to fill all bins beyond the 256×256 case. This ergodicity is strongly suggested by the details shown in Fig. 5, reduced from a large (square-meter) computer-generated plot of 640 000 points. Various logarithmic plots of empty bin fraction as a function of the number of collisions imply that the fraction definitely vanishes for large, but finite, collision numbers (of order 10^9 or so for the 1024×1024 case). This conclusion that no bin is empty is only conjecture, but we believe it to be extremely plausible. If, for instance, the Hausdorff dimension were 1.99 rather than 2.00, this would suggest a number of empty bins, out of 256^2, equal to $256^2[1 - (1/256)^{0.01}]$, which is greater than 3500. Thus, because we found no empty bins we believe that our numerical evidence strongly suggests that the Hausdorff dimension of the attractor is equal to the embedding dimension 2.0 and that the motion is ergodic: All regions of phase space are accessible in this nonequilibrium steady state. Because the occupied phase-space volume is identically zero, these results suggest that the Hausdorff dimension is not a useful concept for describing dynamical attractors. At the same time the *probability* is sufficiently singular (a greater than 2), so that the *occupied* phase space, weighted with its probability, has an information dimension of only $D_1 = 1.8$. The Kaplan-Yorke dimension, which can be estimated from the Lyapunov spectrum and is thought to be equal to the information dimension D_1, is likewise known to be strictly less than the equilibrium phase-space dimension in all deterministic and time-reversible nonequilibrium steady states.[2]

The functions $f(a)$ for three different bin sizes and field strength $3P^2/m\sigma$ are displayed in Fig. 6. The curves summarize 10^8 collisions, collected into 4^n bins,

FIG. 5. Multifractal phase-space probability-density cross section of Fig. 4 but with an enhanced resolution using 640 000 dots on an 8×8 grid. The original computer-generated picture is a 1-m square.

with $n = 8$, 9, and 10. This choice of collision numbers provides 1% or better estimates for the bin-counting dimensions D_q, with $5 \geq q \geq 0$. The spectra show no shoulders, cusps, or fine structure. These results should be compared to those of Morriss, which are reproduced in Fig. 2.

For comparison, and as a check of our numerical work, we show in Fig. 7 exactly the same calculation but carried out at equilibrium, in the absence of an accelerating field. (For technical reasons the data were generated at a field of $0.001P^2/m\sigma$, rather than zero.) The spectrum deviates from the δ-function analytic result ($a = 2$ and $f = 2$) for this system only because the finite-bin populations have fluctuations around their equilibrium values. The phase-space "attractor" cross section is mixing and ergodic at equilibrium with an integrated cross-sectional bin probability varying as δ^2. Thus both a and f should be exactly 2 in this case. The numerical results suggested that fluctuations in bin numbers should lead to inaccuracies in the dimensionality estimates for D_0, D_1, and D_2 less than 1%.

Kaplan and Yorke connected a fractal dimension D_{KY} to the spectrum of Lyapunov exponents, $\{\lambda\} = (\lambda_1, \lambda_2, \lambda_3, \ldots)$. The exponent sums, $\lambda_1, \lambda_1 + \lambda_2, \lambda_1 + \lambda_2 + \lambda_3, \ldots$, describe the exponential time rates of change of 1-, 2-, 3-, . . ., dimensional phase-space objects. Kaplan and Yorke estimated the dimensionality $D_{KY} \approx D_1$ by estimating, with linear interpolation, the dimensionality of a phase-space object in which the exponential rates of change sum to exactly zero. If the underlying Lyapunov exponents used in the Kaplan-Yorke estimate vary in an *analytic* way with the deviation from equilibrium, then one expects to find that the fractal dimension D_{KY} varies *quadratically* with field strength. A

TABLE I. Information and correlation dimensions D_1 and D_2 for 100 000 000 hard-disk collisions using 512×512 bins. The a value corresponding to the correlation dimension $a_2(q=2)$ is shown also. The "fit" results for these dimensions all give the result of a quadratic dependence between zero field and $E = P^2/m\sigma$. For comparison, the results for $E = 3P^2/m\sigma$ are also shown, though these exhibit significant deviation from the small-field quadratic behavior.

	Dimensionless field strength: $Em\sigma/P^2$					
	0.000	0.250	0.500	0.750	1.000	3.000
D_1	2.000	1.998	1.995	1.988	1.979	1.832
Fit	2.000	1.999	1.995	1.988	1.979	1.81[a]
D_2	1.999	1.994	1.980	1.955	1.920	1.583
Fit	2.000	1.995	1.980	1.955	1.920	1.28
a_2	2.000	1.995	1.985	1.966	1.940	1.656
Fit	2.000	1.996	1.985	1.966	1.940	1.46

[a]The extrapolated result for the information dimension D_1 with an infinite number of bins is also 1.81.

linear variation is ruled out by symmetry. The numerical evidence for quadratic dependence, based on the information and correlation dimensions, D_1 and D_2 is shown in Table I. Just as in our "color conductivity" many-body simulations,[8,25] it appears that the one-body far-from-equilibrium Galton board studied here *does* show a quadratic variation of dimensionality for D_1 and D_2.

III. CONCLUSION

The multifractal distributions found here, for the simplest possible mixing and ergodic nonequilibrium atomistic flow, resemble those found in the study of nonlinear dynamical systems. The main difference is the asymmetry of the dependence of fractal dimension $f(a)$, on a, with most of the singularity strength just below the dimensionality of the phase-space cross section 2. At the value of a corresponding to a well-behaved smooth probability density $a = 2$ the corresponding Hausdorff dimension $f(a = 2)$ is about 1.94, significantly less than the embedding dimension.

Experience with molecular-dynamics time-series multifractals is limited, but the lack of symmetry most likely reflects two facts. First, as emphasized by Morriss, atomistic systems are *already* chaotic at equilibrium and become less so, rather than more so, when driven away from equilibrium. Second, because almost all phase-space trajectories obey the second law of thermodynamics,[2] the phase-space singularity strengths tend to be attractive, with dimensionality less than that of the embedding space. Nevertheless, for q less than about $\frac{1}{2}$, the singularity strength is greater than 2, indicating spreading rather than contraction.

The Chhabra-Jensen approach makes accurate calculations possible. Our results show none of the fine structure found by Morriss in his shear-flow simulations. We thought that the reason for this difference could possibly lie in the periodic time dependence of Morriss's shear flow.[12] In that flow the shape of the unit cell passes
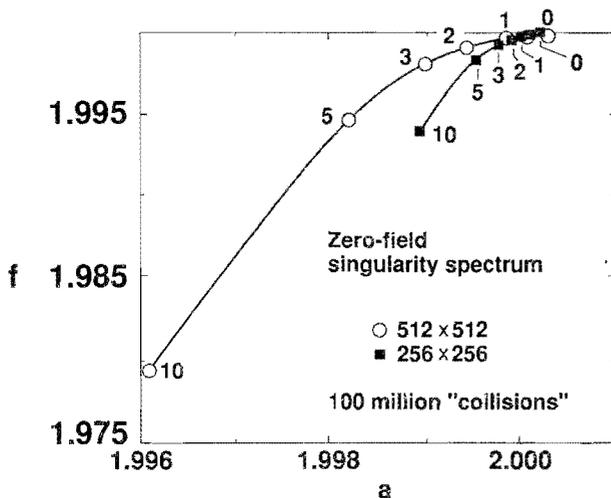

FIG. 7. Apparent spectrum of fractal dimension for the equilibrium situation, with no external field, using 100 000 000 "collisions." The (analytic) known spectrum is a δ function with both averages, $f(a)$ and a equal to the cross-section dimension 2. This result requires infinitesimal bin sizes and an infinitely long sequence of collisions. These zero-field results were generated randomly. Comparison for 100 000 000 collisions shows that the results closely resemble true collision chains for a field of $0.001P^2/m\sigma$.

periodically between rectangular and triangular lattices. This periodic change in symmetry proceeds with a time period equal to the inverse of the shear rate. Formally, this means that the phase space acquires an additional dimension, as is discussed in Ref. 9, a time variable that spans one complete period of the motion. Morriss's average over *all* values of the time *projects* his four-dimensional results onto a three-dimensional subspace from which the time variable is absent, changing the fractal nature of the underlying distributions.

Our own two-body diffusive flow problem exhibits a phase-space singularity structure with the familiar[20] smooth structure leading to a featureless maximum. This qualitative resemblance strongly suggests that the phase-space structures for many-body nonequilibrium flows bear a family resemblance to those found in studies of nonlinear dynamical systems.

It is extremely interesting that the apparent Hausdorff dimension of this strange attractor is 3 in the full phase space (2 in the cross section investigated here), the *same* as that of the embedding space, and in fact, even *filling* the embedding space. By symmetry, those states corresponding to a time reversal of the attractor, the "repeller" (which violates the second law of thermodynamics), have an *exactly similar* distribution (obtained by replacing $\sin\beta$ by $-\sin\beta$). This leads to the perhaps surprising conclusion: Arbitrarily close to every attractor point there is a repeller point and *vice versa*.

The situation is analogous to two nearby lines in three dimensions, but much more complex because the objects which are "close" to each other in the three-dimensional Lorentz-gas phase space have information dimensions just below that of the space itself, 2.8 in the case of a field of strength $3P^2/m\sigma$.

The dynamics of the Lorentz gas is *time reversible*. We believe that this feature is *fundamental* for the phase-space-filling structure found here. Time reversibility is nevertheless neither necessary nor sufficient for ergodicity. The randomness of the Langevin equation establishes that time reversibility is not a *necessary* condition. The Kolmogorov-Arnold-Moser theorem further establishes that time reversibility is not a *sufficient* condition for ergodicity.

Why then, is time reversibility important? Because time-reversible trajectories can in principle be extended either forward or backward in time, time reversibility implies that an initial condition exists somewhere in the finite bounded phase space, which will lead to *any* desired state at *any* desired time in the future or in the past. To see that this guaranteed accessibility makes it plausible that *any* phase-space bin can and will be occupied, suppose a bin were vacant in the steady state, i.e., vacant for all time. The time-reversed dynamics (going *backward in time)* from such a hypothetical vacant bin must eventually converge to the repeller, a widely dispersed multifractional object, looking just like and filling just as many bins as the attractor, and intersecting it along the line $\beta=0$ which corresponds to head-on collisions. (To construct the Galton-board repeller simply reflect the attractor shown in Figs. 4 and 5 about the line $\beta=0$.)

It seems to us highly implausible that the entire past history of any bin could be completely empty. Thus we believe, on the basis of our numerical results, which suggest this conclusion, that the Galton-board motion is ergodic in the full phase space, coming arbitrarily close to any point. This ergodic space-filling motion is very different from Cantor-set examples or the example of Chhabra and Jensen because here the mapping from one collision to the next is both stationary and reversible, shrinking the volume and the information dimension but not the Hausdorff dimension.

We believe that the reversible dynamics studied here, obeying the second law of thermodynamics, leads to the following phase-space properties:

(i) Symmetry breaking in the spectrum of Lyapunov exponents, with the sum negative.

(ii) Ergodic mixing flow, both forward and backward in time.

(iii) Hausdorff dimension equal to the equilibrium embedding dimension.

(iv) Information and correlation dimensions less than the equilibrium dimension with the information dimension related to the thermodynamic dissipation through the Kaplan-Yorke conjecture.

Of these four properties only the first is firmly established. It follows directly from the equations of motion.[2] The remaining three properties are all indicated strongly by the present simulations, though the utility of the Hausdorff dimension for uncountable sets is uncertain. Confirmation for other dynamical systems would be welcome.

It still remains to forge a computational link between the fractal dimensions studied here and the local Lyapunov spectra. Preliminary work in that direction[28] is very promising, but not yet definitive.

Note added in proof. We have now generated the multifractal spectrum of the hard-disk analog of Morriss's soft-disk system. The successive hard-disk trajectories and collisions can be evaluated analytically. The analysis takes place in the three-dimensional "Poincaré cube" describing successive collisions as a function of boundary phase. The resulting spectrum is a featureless curve like that in Fig. 6, but with a maximum of $f=3$. We therefore found no explanation for Morriss's (soft-disk) cusps.

ACKNOWLEDGMENTS

APPENDIX

Imagine a set of N points, sampled from a multifractional object located in an "embedding space." The

points are representative of the object and are imagined to be generated by a deterministic process. Mathematicians introduce the notion of covering balls or hypercubes and define the dimensionality of the underlying object in terms of the cover in the limits that the number of the covering objects and the number of points sampled is large. It is clear that, for a fixed number of points, the covering objects must be much less numerous than the number of points. From the operational point of view we use hypercubes all of the same size, thus introducing (perhaps) a difference between what we call the bin-counting dimension ($q = 0$ in the text) and the capacity or Hausdorff dimension in which a variety of sizes of covering shapes is used.[14]

For example, consider an ordinary object in three-dimensional space. In this intuitive discussion we wish to avoid wildly wrinkled objects with infinite areas or curves of unbounded variation [like $\sin(1/r)$ near the origin, for instance]. Then a three-dimensional solid object requires a number of covering cubes varying as δ^{-3}. A two-dimensional object requires a number of cubes varying as δ^{-2}, and a one-dimensional object (a curve) requires δ^{-1}. It is natural to extend these integer results to define a general fractal dimensionality in the same way. The Sierpinski sponge shown in Fig. 8, for instance, requires 20^n cubes of sidelength $(\frac{1}{3})^n$ for cover, so that its capacity or bin-counting dimensionality D_0 is $\ln 20 / \ln 3 = 2.727$.

To generalize this idea of fractal dimension to multifractals imagine first a fractal set of points in two dimensions. The fractal nature of the points means that the number of points contained in a small bin δ^2 varies as the a power of δ. Evidently (Chhabra and Jensen[20] give a nice example) a can vary from zero (a δ function) to infinity. We might expect, on intuitive grounds, a values between 1 and 2 for the Lorentz-gas problem, but the numerical work shows that larger values are possible. Chhabra and Jensen show that the fractal dimension $f(a)$ of the singular set with strength a can be found by studying the bin-size dependence of the measures defined in the text (moments of the bin occupation numbers). The first moment (proportional to the probability of the bin) gives the information dimension and the second moment the correlation dimension of the multifractal structure.

As a practical matter it is important to estimate the minimum sample size for determining the dimensionalities. Consider, for instance, the numerical characterization of D_0 for a two-dimensional unit square in which all (x,y) values are weighted equally. Divide the square into $Z = \delta^{-2}$ equally-likely-to-be-sampled square zones. To make it likely that, on the average, no cell is empty, the probability of a cell being empty must be less than $1/Z$. This corresponds to a sampling number given by
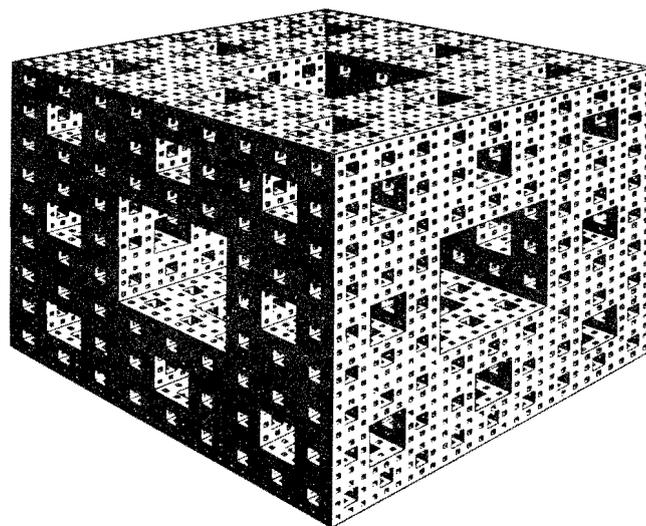

FIG. 8. Sierpinski sponge, with fractal dimension 2.727, obtained by repeatedly removing $\frac{7}{27}$ of the remaining material in an initially homogeneous unit cube.

$$[(Z-1)/Z]^N = 1/Z .$$

Thus a characterization of the Hausdorff dimension for 10^2, 10^4, or 10^6 zones requires roughly 5, 9, and 14 times the number of zones for complete coverage, $N \approx Z \ln Z$.

The Hausdorff dimension, as usually defined, is zero for any set of rational numbers because this "countable" set of $\aleph_o$ elements can be "covered" by lines of length $\delta/2$, $\delta/4$, $\delta/8, \ldots$, summing to δ for δ aribitrarily small. On the other hand, all computer data are finite *and* rational, but certainly the rationals between 0 and 1 "look like" a set of measure 1 rather than 0. Because the mathematics of infinite sets is not operational it can certainly prove useless in some circumstances. It appears to us that the Hausdorff dimension is such a concept for the attractors discussed here.

In the determination of D_0 for the Galton board we soon found that the apparent dimensionality obtained by increasing N at fixed δ would approach the embedding dimension. But for substantially larger grids than 256×256 with a field strength of $3P^2/m\sigma$, it is difficult to generate enough collisions to fill every cell at least once. Statistics for *negative* values of q, which emphasize the sparsely occupied cells are accordingly very poor, except for relatively coarse bins. We therefore have little confidence in fractal dimensions D_q corresponding to negative values of the moment index q and have suppressed them in all the results included in this paper.

[1]For general references, see W. G. Hoover and W. T. Ashurst, Adv. Theor. Chem. **1**, 1 (1975); D. J. Evans and G. P. Morriss, Comput. Phys. Rep. **1**, 297 (1984); *Molecular-Dynamics Simulation of Statistical-Mechanical Systems*, edited by G. Ciccotti and W. G. Hoover (North-Holland, Amsterdam, 1986).

[2]B. L. Holian, W. G. Hoover, and H. A. Posch, Phys. Rev. Lett. **59**, 10 (1987).

[3]S. Nosé, Mol. Phys. **52**, 255 (1984); **57**, 187 (1986); J. Chem. Phys. **81**, 511 (1984).

[4]W. G. Hoover, A. J. C. Ladd, and B. Moran, Phys. Rev. Lett. **48**, 1818 (1982).

[5]W. G. Hoover, *Molecular Dynamics* (Springer-Verlag, Heidelberg, 1986).

[6]Hao Bai-Lin, *Chaos* (World Scientific, Singapore, 1984).

[7]W. G. Hoover and H. A. Posch, Phys. Lett. A **113**, 82 (1985); **123**, 227 (1987).

[8]H. A. Posch and W. G. Hoover, Phys. Rev. A **38**, 473 (1988).

[9]H. A. Posch and W. G. Hoover, Phys. Rev. A **39**, 2175 (1989).

[10]G. P. Morriss, Phys. Rev. A **37**, 2118 (1988).

[11]G. P. Morriss, Phys. Lett. A **134**, 307 (1989).

[12]G. P. Morriss, Phys. Rev. A **39**, 4811 (1989).

[13]B. L. Holian, G. Ciccotti, W. G. Hoover, B. Moran, and H. A. Posch, Phys. Rev. A **39**, 5414 (1989).

[14]D. Farmer, E. Ott, and J. A. Yorke, Physica **7D**, 153 (1983).

[15]K. Pawelzik and H. G. Schuster, Phys. Rev. A **35**, 481 (1987).

[16]W. G. Hoover and A. J. C. Ladd, J. Stat. Phys. **34**, 657 (1984).

[17]W. G. Hoover, K. A. Winer, and A. J. C. Ladd, Int. J. Eng. Sci. **23**, 483 (1985).

[18]A. J. C. Ladd and W. G. Hoover, J. Stat. Phys. **38**, 973 (1985).

[19]G. P. Morris, Phys. Lett. A **122**, 236 (1987).

[20]A. Chhabra and R. V. Jensen, Phys. Rev. Lett. **62**, 1327 (1989).

[21]M. Kac, Sci. Am. **211** (9), 92 (1964).

[22]W. G. Hoover, J. Stat. Phys. **42**, 587 (1986).

[23]B. Moran, W. G. Hoover, and S. Bestiale, J. Stat. Phys. **48**, 709 (1987).

[24]W. G. Hoover, B. Moran, C. G. Hoover, and W. J. Evans, Phys. Lett. A **133**, 114 (1988).

[25]D. J. Evans, W. G. Hoover, B. Failor, and B. Moran, Phys. Rev. A **28**, 1016 (1983).

[26]P. Grassberger, Phys. Lett. A **97**, 227 (1983).

[27]H. G. Hentschel and I. Procaccia, Physica D **8**, 435 (1983).

[28]H. A. Posch (unpublished).